Pharmaceutical Research, Vol. 25, No. 6, June 2008 (© 2008)
DOI: 10.1007/s11095-008-9546-y

Research Paper

A Physiological Model to Evaluate Drug Kinetics in Patients with Hemorrhagic Shock Followed by Fluid Resuscitation

Application to Amoxicillin-clavulanate

Michel Tod,[1,2,3,9,10] Franck Lagneau,[4] Vincent Jullien,[5,6] and Olivier Mimoz[7,8]

Received October 25, 2007; accepted January 24, 2008; published online February 6, 2008

Purpose. To build a physiologically based pharmacokinetic model describing drug kinetics in interstitial fluid in case of hemorrhagic shock, and to propose a simple method to determine the subset of influential parameters that may be estimated with the data at hand.
Methods. The model, which accounts for alterations of regional blood flows and body water distribution, was fitted to amoxicillin and clavulanate kinetic data, assessed in 12 trauma patients with hemorrhagic shock by comparison with 12 healthy volunteers. The predictions were the free concentrations of amoxicillin and clavulanate in 14 organs.
Results. In all tissues of trauma patients, the rate of distribution was lower, but the steady-state level was higher than those in healthy participants. Blood volume was reduced by 25% and blood flow in organs other than lung, brain, and heart were reduced by 18%. Compared with healthy subjects, the time that free amoxicillin concentration remained above 8 mg/L in the interstitial fluid of trauma patients was higher in blood and muscles, and lower in the tendon compartment.
Conclusions. The results and predictions were consistent with the knowledge in this field. The model may be useful to optimize clinical trial designs and drug dosing regimens.

KEY WORDS: amoxicillin; clavulanate; hemorrhagic shock; pharmacokinetics; physiological model.

INTRODUCTION

The influence of shock on the clinical pharmacology of fentanyl (1), remifentanil (2), etomidate (3), and propofol (4) has been documented in animal models. In these examples, shock increased drug concentrations in plasma by several mechanisms: a decrease in blood volume (5) and cardiac output (6,7) along with compensatory changes in regional blood flow and body water distribution (8,9) are the likely physiologic mechanisms explaining the pharmacokinetic changes. However, it remains unclear why the increase in drug concentrations and the associated reduction in dose to achieve the same effect vary widely from one drug to another, ranging from 20% for etomidate to five-fold for propofol in unresuscitated shock (10). Moreover, in clinical practice, fluid resuscitation is provided before the administration of an anesthetic in patients suffering from hemorrhagic shock. Resuscitation restore cardiac output and systemic blood flow and thereby restore in part normal pharmacokinetics as shown for propofol (11). Hence, resuscitation must be accounted for in the optimization of drug dose.

Detailed analysis and understanding of pharmacokinetic–pharmacodynamic changes occuring in patients with hemorrhagic shock followed by fluid resuscitation may benefit from a physiologically-based pharmacokinetic (PBPK) model. These models have demonstrated their usefulness for explaining and/or predicting consequences of changes in body composition and/or blood flows on the pharmacokinetics of e.g. fentanyl, alfentanil (12), thiopental (13) , propofol (14) and cefazolin (15). The aim of the present work was to build a generic PBPK model describing drug kinetics in interstitial fluid in case of hemorrhagic shock followed by fluid

Sources of financial support: EA3738, université Lyon 1, Lyon, F-69003, France.
Work attributed to: Université de Lyon, Lyon, F-69003, France ; université Lyon 1, ISPB, Lyon, F-69008, France.

[1] Pharmacie-Toxicologie, CHU Cochin — Saint-Vincent de Paul, AP-HP, Paris, France.
[2] EA3738, Université de Lyon, Lyon, 69003, France.
[3] ISPB, Université Lyon 1, Lyon, 69008, France.
[4] Département d'anesthésie, CHU Henri Mondor, AP-HP, Créteil, France.
[5] Faculté de Médecine, Université Paris-Descartes, Paris, France.
[6] Service de Pharmacologie Clinique, CHU Cochin — Saint-Vincent de Paul, AP-HP, Paris, France.
[7] Pôle Réanimations Anesthésie, CHU de Poitiers, Poitiers, France.
[8] EA3809 et INSERM ERI-23, Université de Poitiers, 86021, Poitiers, France.
[9] Pharmacie-Toxicologie, Hopital Cochin, 27 rue du Faubourg Saint-Jacques, 75014, Paris, France.
[10] To whom correspondence should be addressed. (e-mail: michel.tod@cch.aphp.fr)

resuscitation, and to propose a simple method to determine the subset of influential parameters that may be estimated with the data at hand. The approach was applied to clinical data gained in a previous study, where the effects of severe trauma with hemorrhagic shock followed by fluid resuscitation on amoxicillin and clavulanate kinetics in plasma was studied by comparison with healthy participants by standard approaches (16).

METHODS

Physiological Model

The physiologically based pharmacokinetic model described by Levitt (17) was used without modifications for healthy volunteers, and modified to account for hemorrhagic shock and fluid resuscitation in patients. In both cases, the model was implemented in ADAPT II (18). The original model has been well validated for xenobiotics remaining in the extracellular space in healthy volunteers (17). Co-amoxiclav and other β-lactamins are antibiotics that remain in the extracellular fluids because they do not penetrate into cells. Briefly, the PBPK model comprises 14 compartments, representing venous blood, arterial blood, lung, portal system (stomach, gut, pancreas, spleen), liver, kidney, heart, brain, muscle, adipose, skin, tendon, bone, and others. Adipose compartment is assumed to contain 80% fat and 20% water. "Tendon" refers to connective tissue, consisting of tendons, cartilage, and subcutaneous tissues. "Bone" refers to the inert solid component of bone that has no volume of distribution or blood flow. The compartments are connected with respect to anatomy.

Each compartment is well mixed. Distribution of the drug is assumed to be restricted to extracellular fluids and could be blood-flow limited or diffusion limited. Albumin is assumed to be the only binding protein, and binding is described as linear (no saturation). Steric and electrostatic exclusion of albumin from the interstitial space is taken into account (19). Elimination is solely by renal route. No distinction is made between glomerular filtration and tubular secretion of the drug.

Each organ *i* is characterized by its mass V_i, extracellular water fraction $wecf_i$ (L/kg), ratio of interstitial to plasma albumin concentration rcP_i, permeability–surface area product for free drug PS_i (L/min/kg), and blood flow Q_i ((L/min/kg). According to Levitt (17), all PS_is are calculated by reference to the free drug PS for muscles, which is the only parameter of this kind to estimate.

The set of standard parameters for a human, as described by Levitt (Table 6 of ref 17, with division of blood volume into arterial, 20%, and venous, 80%), was used: a body weight (BW) of 70 kg, a fat fraction of 0.20 (i.e., 14 kg of fat), a cardiac output of 5.82 L/min, a water content of 42 L, and a mean rcP of 0.28. Interindividual variability of V_i and Q_i was accounted for as follows. The fractional body fat is first determined as (20):

$$\text{fat} = (-10.0 + 1.46\ \text{BMI} - 11.6\ \text{Sex} + 0.14\ \text{Age})/100$$

Then the free fatty mass (FFM) was calculated as BW(1−fat). The organ weights (except adipose) of each subject was calculated as the product of the standard weight by the ratio FFM/56, where 56 is the standard FFM. Water content and blood flow of each organ were adjusted accordingly.

With this model, once the physiological parameters are fixed, the kinetics of the drug is solely determined by clearance of total drug (CL), free drug PS for muscles, and drug binding to albumin (characterized by the free fraction in plasma, fu). When binding is linear, it can be shown that drug kinetics depends only on albumin concentration ratios (rcPs), not on albumin concentration.

Hemorrhagic shock results, by definition, from a blood loss—a reduction in blood volume. This loss may lead to decreased cardiac output and blood flow redistribution among all organs, aiming at maintaining blood flow in heart and brain, while other organs are sacrificed. Restoration of intravascular fluid volume by crystalloids, colloids, plasma, albumin, and blood cells has various effects (21). Crystalloids increase intravascular volume but also extravascular volume by one-third and two-thirds of the infused volume, respectively. This effect vanishes about 1.5 h after the end of infusion. Colloids increase intravascular volume only, and their effect is more prolonged (4 to 24 h). Plasma and albumin infusions restore the concentration of intravascular albumin. Packed red blood cell transfusions increase the hematocrit, reducing the fraction of extracellular water in blood. Platelets are considered to have no hemodynamic effect.

From the physiological model perspective, four parameters are required to describe the changes occurring in patients with hemorrhagic shock: the factor of variation of blood volume (fbl), the factor of variation of the water fraction of blood (fwbl), the factor of variation of extracellular water volume in tissues (fecw), and the factor of reduction of blood flow in all organs except brain, heart, and lung (fq). Variations of the intra- and extravascular water content induce variations of the rcPs by a factor fwbl/fecw. This calculation relies on the observation that albumin equilibrates slowly between intra- and extravascular fluid (19); therefore, the amount of extravascular albumin may be regarded as constant in the time frame of the study.

The model was written as a set of differential equations (described in Appendix). The variability between individuals was handled through (1) the variation of fatty mass and the weight of all organs, (2) the resulting variation of water content and blood flow, (3) the values of CL, fu and the four parameters describing the effect of shock and resuscitation. The physiological parameters were set to their expected value, while the remaining parameters were estimated by fitting the model to the data at hand. Depending on the amount of data, some parameters may or may not be estimated with a reasonable precision. In the following section, a simple method is proposed to determine which parameters are important and the subset of parameters that may be estimated with good precision.

Sensitivity Analysis

A local sensitivity analysis was first conducted to determine the influential parameters in the physiological model: the parameters with a variation that is associated with the largest variation in the disposition curve. For each parameter P of the model, a sensitivity coefficient is calculated as the root mean squared sensitivity brought by all *n* drug concentrations (eventually measured in all tissues) $C(t_j)$ about P as: $\sqrt{(1/n)\sum_{j=1}^{n}\left(\partial C(t_j)/\partial P\right)^2}$. The parameters are then ranked by descending order of sensitivity.

The number of independent parameters, n_p, that may be estimated by fitting the model to e.g. drug concentration in plasma only is twice the number of distinct phases in the disposition curve (a slope and an intercept per phase). The number of distinct phases may be determined as follows. If pharmacokinetics of the drug is linear, the pharmacokinetic model may be written as a sum of exponential terms A_i. exp $(-\alpha_i t)$, i=1 to 14. The parameters A_i and α_i are found by eigenvalue decomposition of the state matrix as described in (22). The contribution of each phase to the area under concentration vs time curve (AUC) is A_i/α_i. Only the phases associated with a contribution greater than 5% may be observed in the disposition curve. The parameters that may be estimated are the n_p first parameters with greater sensitivity.

All these calculations were implemented in the subroutine SPARAM of ADAPT II, by calling appropriate subroutines in the libraries of ADAPT II (18,22).

Patients

The details have been described in a previous publication (16). Briefly, 12 adult patients were enrolled after severe trauma complicated by hemorrhagic shock that justified surgery within 12 h of the trauma. Hemorrhagic shock was defined as the association of at least one episode of systolic blood pressure <90 mm Hg and an intravascular volume expansion >2,000 ml between trauma and surgery. Patients were between 18 and 60 years of age, within 25% of their ideal body weight, and the Injury Severity Score was between 16 and 50. Patients were not included if they had renal failure, defined as creatininemia >150 μM, or cirrhosis, or if they had second- or third degree burns over 10% of their body surface area, or if they were taking drugs known to interfere with co-amoxiclav kinetics.

The volumes of fluids (crystalloids, colloids, fresh-frozen plasma, serum albumin solution) and cells (packed red blood cells, platelets) were recorded separately in the periods before surgery and during surgery.

Healthy Volunteers

Twelve healthy volunteers matched to trauma patients according to age, sex, and body surface area were enrolled.

Antibiotic Treatment

The co-amoxiclav solution (2 g of amoxicillin and 0.2 g of clavulanate) was infused in a peripheral vein over a 30-min period with an infusion pump at the beginning of surgery for the trauma patients and at the start of the pharmacokinetic study for healthy subjects. A second dose was administered 4 h later to trauma patients according to the French consensus conference guidelines (23).

Pharmacokinetic Study

For trauma patients, blood was drawn from the arm contralateral to the antibiotic infusion just before the start of infusion and 10, 15, 30, 35, 45, 60, 90, 120, 180, and 240 min after initiation of the first infusion. For healthy volunteers, the same sampling schedule was used, and two additional samples were taken at 360 and 480 min. Plasma amoxicillin and clavulanate concentrations were measured by liquid chromatography (24,25). For both drugs, the limit of quantification (lowest concentration measured with an imprecision less than 15%) was 1 mg/L, and the coefficient of variation of the assay was less than 13% over the entire calibration range. In the elimination phase, the first concentration less than 1 mg/L was imputed to half the limit of quantification, i.e. to 0.5 mg/L, while the later undetectable concentrations, if any, were removed from the data set.

Parameter Estimation

Because the models for amoxicillin and clavulanate share exactly the same structure, physiological parameter values in a given individual are the same in both models. The only different parameters are the drug-specific parameters, fu and CL. Hence, amoxicillin and clavulanate concentrations versus time data were modeled jointly. The model was implemented as a set of 28 differential equations in ADAPT II (18). The variables were the free concentrations of amoxicillin and clavulanate in each compartment. Parameters were estimated by nonlinear regression. A Bayesian MAP estimator was used to constrain parameter estimates into a plausible range. In healthy volunteers, the factors (fbl, fwbl, fq) were fixed to 1 while fecw was given a prior density N(1,0.2): normal with mean 1 and standard deviation 0.2. In patients, all the factors (fbl, fwbl, fq, and fecw) had a prior density N(1,0.2). For both drugs, the prior density for fu was N(0.8, 0.12), and that for CL was N (0.24, 0.060) in liters per minute. The prior density for fu was defined according to (17) while that for CL was set according to the non-compartmental analysis done in our previous work (16). Finally, the standard deviation of the residual error was related to the predicted concentration by a linear function with positive slope and intercept. The CV of residual error was 15% at 1 mg/L, 6% at 10 mg/L, and 5% at 100 mg/L.

The tissue-to-plasma total drug concentration ratios (Kp_i) and the rate constant for drug diffusion from blood to interstitial space of each organ (k_{Ti}) were calculated as described in Appendix. The volume of distribution at steady-state of total drug was calculated as described by Levitt (17) using the Kps, the water fractions, and the fraction of EDTA interstitial space occupied by the drugs and albumin (see the Appendix).

Goodness-of-fit was assessed by visual examination of the predicted vs observed concentration, and calculation of mean of prediction errors (MPE) and root mean squared prediction error (RMSE). In these calculations, the relative prediction errors (observation–prediction)/prediction were used.

Pharmacodynamic Evaluation

Because the bactericidal effect of co-amoxiclav is related to the time that amoxicillin concentration remains above the MIC (26–28), the time that the amoxicillin free concentration in the extracellular water remained above 8 mg/L (T>8) was calculated for each individual in four representative compartments: venous blood, kidney, muscle, and tendon. This time was expressed as a percentage of the dosing interval (240 min).

Statistical Analysis

Median and range were used as summary statistics. Parameters of trauma patients were compared to those of healthy volunteers using the Mann–Whitney U-test.

RESULTS

Demographics and Treatment

The individual characteristics of healthy volunteers and trauma patients have been detailed in a previous paper (16). Briefly, the mean (SD) age of volunteers and patients was 33 (10) years and 33 (10) years. Their body weight was 73 (10) kg and 76 (11) kg, and their fat proportion was 0.186 (0.058) and 0.219 (0.055), respectively. Creatinine clearance was 107 (30) ml/min and 114 (35) ml/min, respectively. Table I gives the details of the fluid replacement therapy.

Sensitivity Analysis

Preliminary fitting experiments showed that the PS_is were estimated as infinite—i.e., diffusion was a rapid process. Consequently, the model was reduced to a simple blood-flow–limited model, and the PS_is were not considered further.

Setting the physiological and pharmacokinetic parameters to their typical value in healthy volunteers, analysis of the contribution of each phase by eigenvalue decomposition revealed that four phases accounted for 36, 36, 15, and 12%, or 99% of amoxicillin AUC. The half-lives corresponding to these phases (Log $2/\alpha$) were 54, 22, 110, and 1.6 min, respectively. Thus, only four phases could be observed in the disposition curve of amoxicillin.

Results for clavulanate were very close, allowing estimation of eight independent parameters for each drug if the data rendered enough information available. The parameter with the greatest sensitivity was amoxicillin clearance. Setting its sensitivity to 100, the sensitivity was 10 for clavulanate clearance, in the range of 6 to 16 for fus, fbl, fecw and fq, and at 1.5 for fwbl. The sensitivity for all other parameters (Q_i, rcP_i, $wecf_i$) was very low. As a result, it was not possible to gain insight into the physiological modifications specific to each tissue by considering drug concentration in plasma only. The conclusion of these calculations was that our experimental data allowed an estimation of the drug-specific parameters (fu and CL) and four physiological parameters (fbl, fecw, fq, and fwbl). Use of a Bayesian estimator allowed incorporation of prior information into the estimation process, resulting in narrow confidence intervals for these parameters. The standard error of parameter estimates, expressed as a coefficient of variation, was less than 10% for CLs and fus, and less than 20% for the remaining parameters in 22 out of 24 subjects.

Parameter Estimation

The fit was very good in most instances. Two examples are shown in Fig. 1. The mean prediction error and the RMSE were less than 0.02 and 0.12 in 90% of the 48 fits, respectively. The MPE and RMSE of the worst fit were 0.09 and 0.23 for amoxicillin, and 0.11 and 0.26 for clavulanate. The summary of parameter estimates is given in Table II. The mean parameters CL and Vss were in very good agreement with our previous analysis based on a two-compartment model (16). The mean factor of modification of extracellular water volume (fecw) was significantly different from unity in healthy volunteers (P=0.03). This parameter was also significantly greater in trauma patients than in healthy subjects. As a result, the Vss values of amoxicillin and clavulanate were also greater, although the difference did not reach significance. However, there was no correlation between fecw and the extravascular expansion due to fluids administered. There were significant reductions in blood volume and blood flow rate in organs other than brain, heart, or lung.

Table III gives the key parameters describing the distribution of co-amoxiclav in tissues of a typical individual having the mean parameters of either healthy participants or trauma patients. The k_Ts characterize the rate of distribution, while the Kps are related to the steady-state total concentration reached in the interstitial fluid of the tissues. The tissues can be separated into four categories according to their rate constant k_T in healthy individuals: lung and kidney (k_T> 15 min^{-1}); blood, portal, liver, brain, and heart (k_T 1 to 6 min^{-1}); skin, muscle, and adipose (k_T 0.1 to 0.15 min^{-1}); and tendon and other (k_T 0.007 to 0.02 min^{-1}). In trauma patients, fu, fu_Ts, and Kps were increased, while k_Ts were decreased compared to healthy subjects.

Table I. Volume of Fluids Received by Each Patient Before/during the First Dosing Interval of Co-amoxiclav Administration

Patient	Crystalloid (L)	Colloid (L)	Plasma (L)	Packed RBC Units	Albumin (L)	Intravascular Expansion (L)	Extravascular Expansion (L)	Interval[a] (h)
p6	1.3/1.5	5/1	2/1.25	7/4	0/0	7.43/2.75	0.87/1.00	10.33
p7	1.5/0.7	1.5/1	0/1	3/2	0/0	2.00/2.23	1.00/0.47	8.5
p8	0/5.5	5.5/1	2.75/2	13/3	0/0	8.25/4.83	0.00/3.67	10.75
p9	1.5/3	2/1	0.5/0	3/4	0/0	3.00/2.00	1.00/2.00	8.08
p10	3/1.5	2/0	0/0.75	5/4	0/0	3.00/1.25	2.00/1.00	7
p11	0.5/4	3/1	1/0	9/6	0/0	4.17/2.33	0.33/2.67	5.16
p12	0.5/1.5	3/1	1.25/2.5	16/10	0/0.5	4.42/4.50	0.33/1.00	3.5
p16	2.5/3	3/0.5	1/1.75	6/10	0/0	4.83/3.25	1.67/2.00	9.3
p17	1.5/2.5	1.5/3	1/0.75	4/6	0/0	3.00/4.58	1.00/1.67	9.67
p18	2/2.5	2/0	0/0	0/2	0/0	2.67/0.83	1.33/1.67	8.5
p19	3/1.5	3/2.5	2/0	6/6	0/0	6.00/3.00	2.00/1.00	11.5
p20	2/2.5	1/0.5	0/0	0/0	0/0	1.67/1.33	1.33/1.67	10.5

[a] Interval between admission and first administration of co-amoxiclav

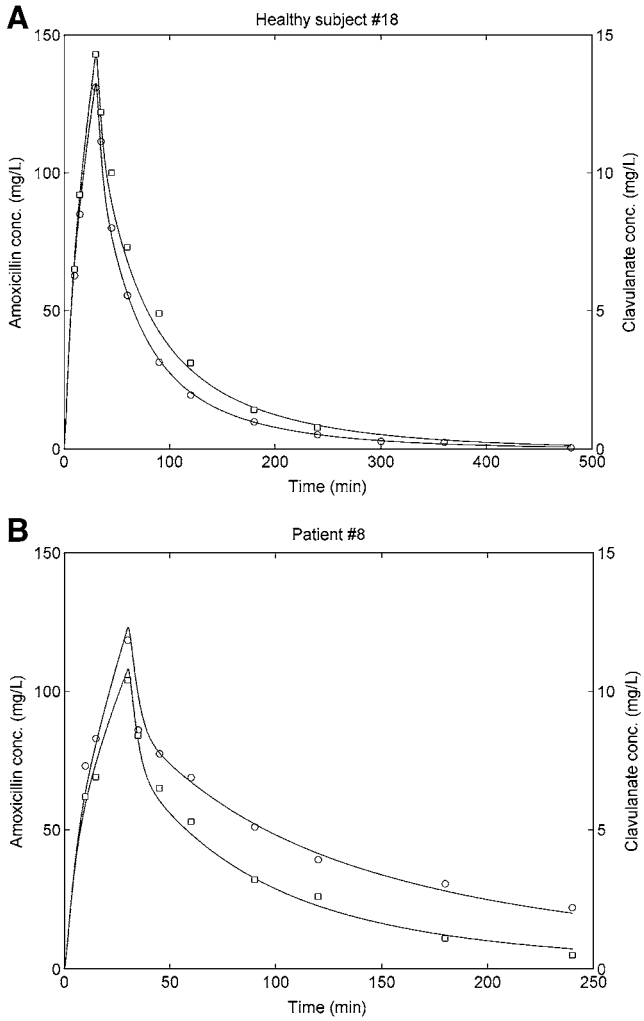

Fig. 1. Two examples of the fit of amoxicillin (*circles*) and clavulanate (*squares*) data. **A** Healthy subject # 18. **B** Patient # 8.

Pharmacodynamic Analysis

Table IV shows the mean (SD) of percent time that free amoxicillin concentration remained above 8 mg/L (T>8) during the dosing interval in interstitial fluid of four representative tissues (one of each category as defined by k_T). A comparison of these times in trauma patients to those in healthy volunteers showed that they were similar in the kidney, significantly longer in blood and in muscles, and shorter in the tendon compartment of trauma patients. In one trauma patient (# 7), T>8 was equal to zero in tendon extracellular water because the entire concentration profile was under 8 mg/L. Excluding this patient from the calculations had no major impact on the results.

The simulation of free amoxicillin concentration kinetics in the extracellular water of four representative tissues of a typical healthy volunteer is shown in Fig. 2. Figure 3 shows the same plot for two trauma patients, one with lower concentration profiles, the other with higher concentration profiles compared with the pattern of the typical healthy individual.

DISCUSSION

Scope of the Model

In its present form, the scope of the PBPK model is restricted to drugs that remain in extracellular fluids, binds linearly to albumin, and are eliminated by renal route. All these restrictions may be overcome, provided that the physiological informations characterizing drug binding to intra- and extracellular macromolecules are known. For example, a very detailed PBPK model for ciclosporine, a drug with intracellular penetration, non-linear binding in blood and tissues, binding to lipoproteins, and hepatic saturable clearance has been described and validated (29) and could inspire extensions of the present model.

Structure of the Model

In this study, the pharmacokinetics of amoxicillin and clavulanate in the interstitial fluid of the main organs were derived by using a physiologically based pharmacokinetic model. This model had been previously validated for amoxicillin in healthy volunteers. It has been extended to accommodate modifications resulting from hemorrhagic shock and its treatment. This model was primarily intended to describe drug distribution in detail, while clearance was accounted for by a single parameter. No attempt was made to model the effects of hemorrhagic shock on clearance because clearance could be readily estimated owing to the high number of plasma levels available. Likewise, we did not attempt to model precisely the effects of colloids or crystalloids, for example, because initial blood volume and blood losses during conditioning and surgery could not have been assessed. Moreover, the sensitivity analysis showed that eight parameters at most could be estimated by using concentra-

Table II. Median (range) and SD of Parameter Estimates of Co-amoxiclav in Both Groups

Parameter	Healthy Participants	Trauma Patients	*P*
fu amox	0.77 (0.62–0.82), 0.06	0.79 (0.66–0.94), 0.06	0.18
CL amox (L/min)	0.25 (0.15–0.40), 0.03	0.21 (0.08–0.40), 0.09	0.06
fu clav	0.84 (0.73–0.90), 0.05	0.82 (0.78–0.91), 0.04	0.29
CL clav (L/min)	0.27 (0.15–0.43), 0.08	0.22 (0.11–0.40), 0.08	0.18
fecw	1.09 (0.85–1.29), 0.12	1.38 (0.58–2.55), 0.52	0.03
fwbl	1	1.03 (0.63–1.07), 0.12	0.55
fbl	1	0.75 (0.51–1.17), 0.20	0.04
fq	1	0.82 (0.34–1.10), 0.26	0.005
Vss amox (L/kg)	0.25 (0.17–0.30), 0.03	0.29 (0.14–0.55), 0.11	0.35
Vss clav (L/kg)	0.26 (0.22–0.32), 0.03	0.29 (0.14–0.48), 0.09	0.75

Table III. Rate Constant for Free Amoxicillin and Tissue-to-plasma Total Concentration Ratio of Amoxicillin in Each Tissue

Compartment	Free Fraction fu or fuT		Rate Constant kT (min^{-1})		Kp	
Venous blood	0.76	0.80	1.3	1.3	0.519	0.509
Arterial blood	0.76	0.80	5.4	5.2	0.519	0.509
Lung	0.91	0.94	37	22	0.154	0.202
Portal	0.91	0.94	1.8	1.0	0.225	0.296
Liver	0.87	0.92	3.0	1.7	0.161	0.209
Kidney	0.91	0.94	17	9.7	0.127	0.167
Brain	0.97	0.98	2.1	1.6	0.144	0.194
Heart	0.87	0.92	2.2	1.7	0.200	0.259
Skin	0.93	0.96	0.12	0.068	0.450	0.597
Muscle	0.87	0.92	0.11	0.060	0.117	0.152
Adipose	0.91	0.94	0.12	0.067	0.193	0.253
Tendon	0.93	0.96	0.0069	0.0038	0.796	1.06
Other	0.93	0.96	0.017	0.0096	0.637	0.846

In each cell of the table, the first value is for a typical healthy volunteer, the second value for a typical trauma patient. BW=70 kg, fat=0.20. Other parameters are the median parameters of Table II

tions measured in plasma only. Lumping physiological models (*i.e.*, aggregation of a number compartments with similar kinetic behavior) has been suggested to reduce the number of parameters and increase the ability to estimate the remaining parameters (30). However, in the context of our study, lumping was *a priori* impossible because compartments with similar kinetic behavior may differ between the healthy participants and trauma patients, leading to different model reductions. For these reasons, the full model was used for analyzing the data from both populations.

Parameter Estimates

Elimination clearance and Vss estimates obtained by fitting the PBPK model were very close to those obtained by conventional approaches in our previous study (16). In healthy volunteers, the median factor controlling extracellular water volume was 1.09 instead of the expected value of 1, which may indicate a moderate model misspecification (see Table II). Nevertheless, this parameter was increased to 1.38 in trauma patients, showing that patients had volume of extracellular fluids that was 1.27 times (1.38/1.09) higher than that of healthy subjects. On the other hand, blood volume at the time of surgery was reduced by 25% (fbl=0.75 versus 1), and blood flows in organs other than lung, brain, and heart were reduced by 18% (fq=0.82 versus 1). From a qualitative point of view, these results were expected, but the PBPK model allows a quantitative description of the physiological modifications.

It is instructive to compare these results with those of our previous analysis based on a two-compartment model (16). With this previous model, we found that the central volume of distribution was reduced by a factor 2.5, while the volume of peripheral compartment and clearance of distribution were increased by 2 and 3.5, respectively. The present analysis with the PBPK model showed no equivalent modifications and ruled out an increased rate of distribution (the PS_i values were infinite; distribution was blood flow-limited). On the contrary, we conclude that rate constants of distribution in tissues are reduced. This discrepancy might be explained by the fact that the two-compartment model cannot be interpreted in a physiological way because it is not possible to properly reduce the PBPK model to a two-compartment model; the k_T values of all organs are too widely different (30).

Pharmacodynamic Analysis

The main pharmacokinetic result from the PBPK model is that in trauma patients, the rate constants of distribution in tissues are reduced while the steady-state free concentrations are increased. Hence, if the drug were administered by continuous infusion, reaching the steady-state would take longer, but the steady-state value would be higher. Because the drug was administered by short infusion, its concentration could decline before the steady-state concentration was reached. Thus, the time that the free concentration remains above a given threshold may increase or decrease depending

Table IV. Median (range) of Percent Time that Free Amoxicillin Concentration Remained Above 8 mg/L During Dosing Interval

Compartment	Healthy participants	Trauma patients	*P*
Kidney	57 (46–82)	64 (18–99)	0.32
Venous blood	71 (64–94)	83 (56–100)	0.007
Muscle	73 (66–96)	89 (68–98)	0.001
Tendon	90 (89–93)	86 (0–93)	0.010
		85 (67–93)[a]	0.019

[a] One null value (patient # 7) excluded in the trauma patients group

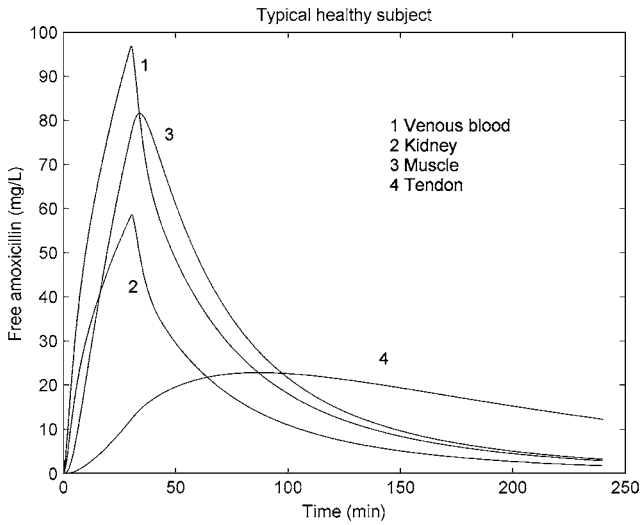

Fig. 2. Simulation of free amoxicillin concentration kinetics in the extracellular water of four representative tissues of a typical healthy volunteer (body weight, 73 kg, fat fraction=0.186).

on the k_T and the Kp of the tissue. For greater discrimination, the threshold was fixed to a high value (8 mg/L), which is higher than the breakpoint for resistant strains (4 mg/L) determined *in vivo* in an animal model of *Streptococcus pneumoniae* infection (26).

The simulations showed that for trauma patients compared with healthy subjects, the T>8 was longer in most tissues but might be shorter in tendon, a compartment with low k_T. Moreover, there was a large interindividual variability in the exposure, so that one patient among 12 had a T>8 equal to zero in tendon. This outcome was probably not detrimental because the concentration increased above the threshold after the second dose (simulation not shown). For the other tissues, T>8 was greater than 60% of the dosing interval in all patients. In animal or *in vitro* pharmacodynamic models, co-amoxiclav has been shown to reach maximal antibacterial effect when amoxicillin T>MIC was greater than 40%–50%[26] or 50%–60% of the dosing interval (31). Therefore, co-amoxiclav should have a maximal effect for strains with a MIC up to 8 mg/L in trauma patients with hemorrhagic shock, and the pharmacokinetic differences between healthy subjects and trauma patients shown in Table IV are not important from a clinical point of view.

Validation of the Model

It is important to distinguish the results and the inferences. The results corresponds to parameter estimates (Tables II and III, Fig. 1) and the inferences to simulations (Table IV and related figures). The results are based on experimental data (drug concentrations measurements in plasma), physiological data obtained in different studies (organ volumes, blood flows,…) and on physiological and mathematical principles. Provided that these principles are considered as sound and the physiological data are appropriate for the subjects studied here, the sensitivity analysis ensures that all the parameter estimates obtained by fitting the model to the available data, although limited to concentrations in plasma, were obtained with reasonable precision and accuracy. The similarity of Vss estimates obtained with the PBPK model and the non-compartmental approach supports this contention.

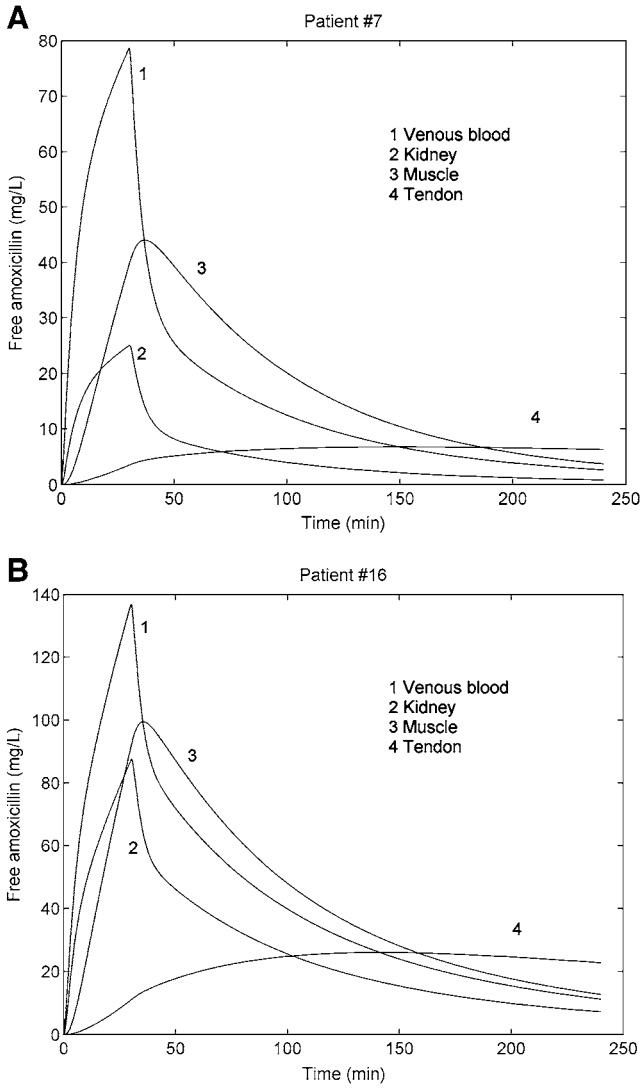

Fig. 3. Simulation of free amoxicillin concentration kinetics in the extracellular water of four representative tissues of two extreme patients. **A** Patient # 7. **B** Patient # 16.

The inferences are the simulations of free drug concentration profile in the tissues, made from measurements of total dug concentration. These may be regarded as speculative and requiring experimental validation. However, direct measurements of free antibiotic concentration in interstitial fluids by microdialysis are not appropriate for rapidly changing concentrations because a 10–30-min delay is required for sample collection (32,33). Measurement of concentrations in surgically excised tissues results in underestimation of the true concentration of antibiotics restricted to the extracellular space because of the dilution induced by tissue homogenization (34,35). This dilution is expected to be variable in case of fluid resuscitation and cannot be easily accounted for. A powerful method for the validation of PBPK model predictions is positron emission tomography (e.g. (36)) which allows to determine drug kinetics in organs. This method does not distinguish intracellular and interstitial concentrations but, at

least for drugs that do not penetrate into cells, could allow a direct validation of the model.

In summary, the proposed PBPK model allowed a quantitative description of the physiological modifications underlying changes of drug pharmacokinetics in hemorrhagic shock followed by fluid resuscitation. To overcome the usual difficulty due to overparametrization of PBPK models, a simple method has been proposed to determine which parameters are important and the subset of parameters that may be estimated with good precision, depending on the experimental data at hand. Application of this approach to amoxicillin and clavulanate pharmacokinetic data yielded results and predictions consistent with the knowledge in this field. Simulations of the model may be useful to optimize clinical trial designs and drug dosing regimens.

APPENDIX: EQUATIONS OF THE MODEL

Base Model

A description of the model equations is presented here. More details and explainations may be found in the article of Levitt (17). The model is written as set of differential equations. Each equation describes the variation of the free drug concentration in the interstitial fluid of an organ (compartment). Each organ *i* is characterized by its mass V_i (kg), extracellular water fraction $wecf_i$ (L/kg), ratio of interstitial to plasma albumin concentration rcP_i, permeability–surface area product PS_i for free drug (L/min per kg of organ), and blood flow Q_i (L/min per kg of organ).

The unbound fraction of drug in the volume of interstitial fluid (assimilated to the EDTA space) of each organ, fu_{Ti}, is calculated as :

$$fu_{Ti} = \frac{1}{1 + \text{Kass}.(rcP_i/\alpha_i) \cdot \text{Prot}}$$

where Kass is the association constant for drug binding to albumin measured in plasma (L/mol), Prot is albumin concentration in plasma (mol/L), and α_i is the fraction of EDTA interstitial space accessible to the drug in organ i. This parameter allows to take into account steric of electrostatic exclusion of the drug from the interstitial space.

In case of permeability-limited diffusion of the drug into the interstitial space of an organ, the fraction of the arterial drug concentration that diffuses into interstitial fluid during a single pass is calculated as:

$$fclear_i = 1 - \exp\left(-\frac{fu_b \cdot PS_i}{1.06\ wecf_b \cdot Q_i}\right)$$

where fu_b is the free fraction of drug in the blood, $wecf_b$ the water fraction of blood in L/kg, and 1.06 is the density of blood in kilograms per liter.

The rate constant for free drug diffusion from blood to interstitial space of each organ, in 1/min, is calculated as:

$$k_{Ti} = 1.06\ fclear_i \cdot \frac{fu_{Ti} \cdot wecf_b \cdot Q_i}{fu_b \cdot wecf_i}$$

This equation may be viewed as the ratio of an unbound drug distribution clerarance $(1.06\, wecf_b \cdot Q_i \cdot V_i/fu_b)$ to an unbound drug volume of distribution $(V_i \cdot wecf_i/fu_{Ti})$.

The generic equation describing the variation of the free drug concentration in the interstitial fluid of an organ (Cu_{Ti}) is:

$$\frac{dCu_{Ti}}{dt} = k_{Ti}(Cu_A - Cu_{Ti}) - ke.Cu_{Ti}$$

where Cu_A is the free drug concentration in arterial blood, and ke is an elimination rate constant, if any. This rate constant is calculated as the ratio of an unbound drug elimination clerarance $(1.06\ wecf_b \cdot CLi/fu_b)$ to an unbound drug volume of distribution $(V_i \cdot wecf_i/fu_{Ti})$. CLi is the intrinsic clearance of total drug, related to the organ clearance CL_{org} by a clearance model. In the simple case of a well mixed model, the relationship is:

$$CLi = \frac{CL_{org}}{1 - (CL_{org}/Q_{org})}$$

The tissue-to-plasma total drug concentration ratios (Kp_i) are calculated as:

$$Kp_i = \frac{fu.wecf_i}{0.94\ fu_{Ti}}$$

where 0.94 is the water fraction of plasma in liters per kilogram.

The volume of distribution of total drug at steady-state is calculated as:

$$Vss = Vp + \sum_1^n \alpha_i \cdot V_i \cdot wecf_i \cdot \left(\lambda_E \cdot \frac{fu_p}{fu_{Ti}} + (1 - \lambda_E) \cdot fu_p\right)$$

where Vp is the volume of water in plasma, λ_E is the fraction of interstitial volume (EDTA space) accessible to albumin (λ_E=0.45), and the sum is over the *n* organs.

Characterization of Hemorrhagic Shock and Fluid Resuscitation

The following changes are made to the base model. The volumes (V_i) of venous and arterial blood are multiplied by the factor of variation of blood volume (fbl). The extracellular water fractions ($wecf_i$) are multiplied by the factor of variation of the water fraction of blood fwbl (venous and arterial blood) or the factor of variation of extracellular water volume fecw (other tissues). The ratios of albumin concentration (rcP_i) are multiplied by a factor fwbl/fecw. The blood flows (Q_i) are multiplied by the factor of reduction of blood flow (fq) in all organs except brain, heart, and lung.

REFERENCES

1. T. D. Egan, S. Kuramkote, G. Gong, J. Zhang, S. W. McJames, and P. L. Bailey. Fentanyl pharmacokinetics in hemorrhagic shock: a porcine model. *Anesthesiology* **91**:156–166 (1999).
2. K. B. Johnson, S. E. Kern, E. A. Hamber, S. W. McJames, K. M. Kohnstamm, and T. D. Egan. Influence of hemorrhagic shock on

remifentanil: A pharmacokinetic and pharmacodynamic analysis. *Anesthesiology* **94**:322–332 (2001).
3. K. B. Johnson, T. D. Egan, J. Layman, S. E. Kern, J. L. White, and S. W. McJames. The influence of hemorrhagic shock on etomidate: A pharmacokinetic and pharmacodynamic analysis. *Anesth. Analg.* **96**:1360–1368 (2003).
4. K. B. Johnson, T. D. Egan, S. E. Kern, J. L. White, S. W. McJames, N. Syroid, D. Whiddon, and T. Church. The influence of hemorrhagic shock on propofol: A pharmacokinetic and pharmacodynamic analysis. *Anesthesiology* **99**:409–420 (2003).
5. T. Kazama, K. Ikeda, K. Morita, T. Ikeda, M. Kikura, S. Sato. Relation between initial blood distribution volume and propofol induction dose requirement. *Anesthesiology* **94**:205–210 (2001).
6. T. Kurita, K. Morita, T. Kazama, and S. Sato. Influence of cardiac output on plasma propofol concentrations during constant infusion in swine. *Anesthesiology* **96**:1498–1503 (2002).
7. R. N. Upton, G. L. Ludbrook, C. Grant, and A. M. Martinez. Cardiac output is a determinant of the initial concentrations of propofol after short-infusion administration. *Anesth. Analg.* **89**:545–552 (1999).
8. A. R. Edouard, A. C. Degremont, J. Duranteau *et al*. Heterogeneous regional vascular responses to simulated transient hypovolemia in man. *Intensive Care Med.* **20**:414–420 (1994).
9. W. C. Schoemaker. Circulatory mechanisms of shock and their mediators. *Crit. Care Med.* **15**:787–794 (1987).
10. S. L. Shafer. Shock values. *Anesthesiology* **101**:567–568 (2004).
11. K. B. Johnson, T. D. Egan, S. E. Kern, M. L. Cluff, and N. L. Pace. Influence of hemorrhagic shock followed by crystalloid resuscitation on propofol: A pharmacokinetic and pharmacodynamic analysis. *Anesthesiology* **101**:647–659 (2004).
12. S. Bjorkman, D. R. Wada, and D. R. Stanski. Application of physiologic models to predict the influence of changes in body composition and blood flows on the pharmacokinetics of fentanyl and alfentanil in patients. *Anesthesiology* **88**(3):657–667 (1998).
13. D. R. Wada, S. Bjorkman, W. F. Ebling, H. Harashima, S. R. Harapat, and D. R. Stanski. Computer simulation of the effects of alterations in blood flows and body composition on thiopental pharmacokinetics in humans. *Anesthesiology* **87**(4):884–899 (1997).
14. R. N. Upton, and G. Ludbrook. A physiologically based, recirculatory model of the kinetics and dynamics of propofol in man. *Anesthesiology* **103**(2):344–352 (2005).
15. F. Lagneau, J. Marty, P. Beyne, and M. Tod. Pharmacokinetic evaluation of the french recommended protocol for antibioprophylaxis during liver surgery: A physiological modeling approach. *J. Pharmacokinet. Pharmacodyn.* **32**(1):1–32 (2005).
16. O. Mimoz, V. Schaeffer, P. Incagnoli, K. Louchahi, A. Edouard, O. Petitjean, and M. Tod. Co-amoxiclav pharmacokinetics during post-traumatic hemorrhagic shock. *Crit. Care Med.* **29**:1350–1355 (2001).
17. D. G. Levitt. The pharmacokinetics of the interstitial space in humans. *BMC Clin. Pharmacol.* **3**:3 (2003).
18. D. Z. D'Argenio, and A. Schumitzky. *ADAPT II User's Guide: Pharmacokinetic/Pharmacodynamic Systems Analysis Software*. Biomedical Simulations Resource, Los Angeles, 1997.
19. C. C. Gyenge, O. Tenstad, and H. Wiig. *In vivo* determination of steric and electrostatic exclusion of albumin in rat skin and skeletal muscle. *J. Physiol.* **552**(Pt 3):907–916 (2003).
20. D. Gallagher, M. Visser, D. Sepulveda, R. N. Pierson, T. Harris, and S. B. Heymsfield. How useful is body mass index for comparison of body fatness across age, sex, and ethnic groups? *Am. J. Epidemiol.* **143**:228–239 (1996).
21. G. Gutierrez, H. D. Reines, and M. E. Wulf-Gutierrez. Clinical review: hemorrhagic shock. *Crit. Care* **8**(5):373–381 (2004).
22. D. Z. D'Argenio, A. Schumitzky, and W. Wolf. Simulation of linear compartment models with application to nuclear medicine kinetic modeling. *Comput. Methods Programs Biomed.* **27**(1):47–54 (1988).
23. Société Française d'Anesthésie et de Réanimation. Consensus conference. "Antibioprophylaxis in a surgical setting." 10–11 December 1992, Faculté de Médecine Xavier Bichat. *Cah. Anesthesiol.* **41**:273–280 (1993).
24. M. Foulstone, and C. Reading. Assay of amoxicillin and clavulanic acid in biological fluids with high-performance liquid chromatography. *Antimicrob. Agents Chemother.* **22**:753–776 (1982).
25. P. Leroy, C. Gavriloff, A. Nicolas, *et al*. Comparative assay of amoxicillin by high-performance liquid chromatography and microbiological methods for pharmacokinetic studies in calves. *Int. J. Pharm.* **82**:157–164 (1992).
26. D. Andes, and W. A. Craig. *In vivo* activities of amoxicillin and amoxicillin-clavulanate against *Streptococcus pneumoniae*: application to breakpoint determinations. *Antimicrob. Agents Chemother.* **42**(9):2375–2379 (1998).
27. S. Bronner, V. Murbach, J. D. Peter, D. Leveque, H. Elkhaili, Y. Salmon, N. Dhoyen, H. Monteil, G. Woodnutt, and F. Jehl. *Ex vivo* pharmacodynamics of amoxicillin-clavulanate against beta-lactamase-producing *Escherichia coli* in a yucatan miniature pig model that mimics human pharmacokinetics. *Antimicrob. Agents Chemother.* **46**(12):3782–3789 (2002).
28. S. Bronner, D. Pompei, H. Elkhaili, N. Dhoyen, H. Monteil, and F. Jehl. *Ex vivo* 12 h bactericidal activity of oral co-amoxiclav (1.125 g) against beta-lactamase-producing *Haemophilus influenzae*. *J. Antimicrob. Chemother.* **48**(4):501–506 (2001).
29. R. Kawai, D. Mathew, C. Tanaka, and M. Rowland. Physiologically based pharmacokinetics of cyclosporine A: extension to tissue distribution kinetics in rats and scale-up to human. *J. Pharmacol. Exp. Ther.* **287**(2):457–468 (1998).
30. I. A. Nestorov, L. J. Aarons, P. A. Arundel, and M. Rowland. Lumping of whole-body physiologically based pharmacokinetic models. *J. Pharmacokinet. Biopharm.* **26**(1):21–46 (1998).
31. A. P. MacGowan, A. R. Noel, C. A. Rogers, and K. E. Bowker. Antibacterial effects of amoxicillin-clavulanate against *Streptococcus pneumoniae* and *Haemophilus influenzae* strains for which MICs are high, in an *in vitro* pharmacokinetic model. *Antimicrob. Agents Chemother.* **48**(7):2599–2603 (2004).
32. L. Heinemann. Glucose Monitoring Study Group: Continuous glucose monitoring by means of the microdialysis technique: Underlying fundamental aspects. *Diabetes Technol. Ther.* **5**:545–561 (2003).
33. S. H. Khan, and A. Shuaib. The technique of intracerebral microdialysis. *Methods* **23**:3–9 (2001).
34. D. E. Nix, S. D. Goodwin, C. A. Peloquin, D. L. Rotella, and J. J. Schentag. Antibiotic tissue penetration and its relevance: models of tissue penetration and their meaning. *Antimicrob. Agents Chemother.* **35**(10):1947–1952 (1991).
35. D. E. Nix, S. D. Goodwin, C. A. Peloquin, D. L. Rotella, and Schentag. Antibiotic tissue penetration and its relevance: impact of tissue penetration on infection response. *Antimicrob. Agents Chemother.* **35**(10):1953–1959 (1991).
36. M. Brunner, O. Langer, G. Dobrozemsky, U. Muller, M. Zeitlinger, M. Mitterhauser, W. Wadsak, R. Dudczak, K. Kletter, and M. Muller. [18F]Ciprofloxacin, a new positron emission tomography tracer for noninvasive assessment of the tissue distribution and pharmacokinetics of ciprofloxacin in humans. *Antimicrob. Agents Chemother.* **48**(10):3850–3857 (2004).